Effects of nanomaterial properties on the effective conjugation of antiviral drugs

Ismail Adwibi[1], Peng Zhang[1], Laura-Jayne A. Ellis[1], Sophie M. Briffa[1], Eugenia Valsami-Jones[1]

[1]Department of Geography, Earth and Environmental Sciences, University of Birmingham, Birmingham, UK

Introduction

- In 2019, a novel coronavirus known as SARS-CoV-2 set off a new disease, COVID-19, which has since caused a global pandemic. Many research areas have been directly or indirectly impacted by this pandemic. Medical facilities around the world, for example, have reassigned all available resources to address this global disaster and its implications on our everyday life (Figure 1). Other research fields have also been affected, from environmental science, where positive changes in environmental quality have been observed from reduced traffic during lockdowns, to human health, where a negative impact on mental and physical health have been widely observed. Moreover, this global pandemic has brought a severe global economic crisis that has not been witnessed before since the 2nd world war.

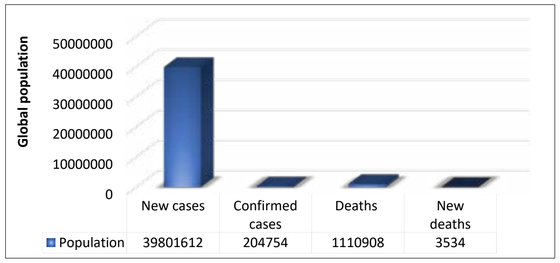

Figure 1. Coronavirus disease (COVID-19) global health statistics updated by world health organisation (WHO) on 19th – October 2020 (source: world health organisation) [1].

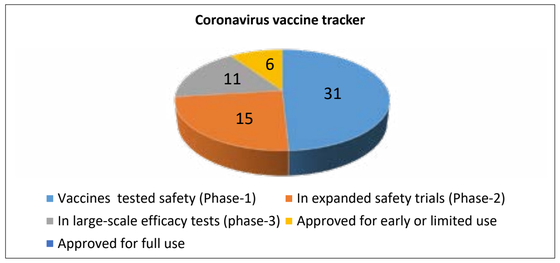

Figure 2. Efforts for development of novel vaccines since pandemic starts (source: New York Times) [2].

- Currently governments around the world have spent billions of dollars for the treatment of those most severely affected and, in parallel, there are significant efforts around the world to develop a novel vaccine and/or antiviral therapeutics (Figure 2).
- Meanwhile, nanotechnology, as a broad range enabling technology, has facilitated the development of a multitude of medical solutions. Notably, engineered nanomaterials (ENMs) due to their unique physicochemical properties, make ideal candidates for therapeutic interventions, including those required for targeting a virus or its systemic effects. Examples include: a) nanobodies with high specificity to the virus machinery, in the case of SARS-CoV-2 its spike protein, which can act to block entry into cells or b) tailor made ENMs, which can be used as carriers of virus-active biomolecules.

Objectives

- In this work we are focusing on gold nanoparticle (AuNP) synthesis with the aim to facilitate control of optimal delivery of antiviral treatments.
- We are specifically systematically varying particle size to identify a size range that is optimal to carry a maximum drug load, maintain this load (and avoiding acid or enzymatic degradation or hydrolysis) and delivering it to the target organ in the body.

Materials and methods

Materials:

Chloroauric acid ($HAuCl_4$), sodium citrate (Na-Cit), bovine serum albumin (BSA), 4-mercaptobenzoic acid (4-MBA), 11-mercaptoundecanoic acid (MUDA), Tannic acid (TA), phosphate buffer saline (PBS) at pH 7.4.

Citrate reduction method:

AuNPs with size approximately 15 nm in diameter have been synthesized as reported by briefly, $HAuCl_4$ (1mM) boiled at 100°C for a period of time. Then sodium citrate was added quickly. The color changed in few minutes from light yellow to deep-wine red leading to formation of gold nanoparticles [6].

Synthesis of gold nanoparticles up to 100 nm in diameter:

This was conducted by using the seed growth solution method [6]. Briefly, 149 mL of sodium citrate (2.2mM) was mixed with 1 mL of tannic acid, TA (5mM). Then, the mixture was boiled at around 70 °C. After, 1 mL of $HAuCl_4$ (25mM) was injected. Then first seed solution was extracted and replaced with same amount of Na-Cit (2.2mM). The process repeated until the targeted size was obtained.

Binding of bovine serum albumin (BSA) to AuNPs:

Conjugation of protein (BSA) was studied as reported in the published work by Wu et al. with some modifications [4]. The conjugation involves the use of BSA with different concentrations at fixed cit-AuNPs. (see schematic1)

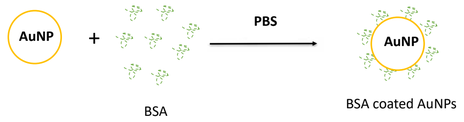

Schematic 1. Binding of bovine serum albumin (BSA) to cit-AuNPs.

Conjugation of 4-MBA with cit-AuNPs:

4-mercaptobenzoic acid functionalized AuNPs were synthesized as reported with minor modifications [3].

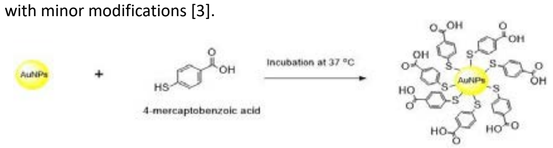

Schematic 2. Conjugation of 4-mercaptobenzoic acid to cit-AuNPs (Chemdraw 19.1).

Results and Discussion

UV-Vis spectroscopy:

Herein, all ultraviolet-visible (UV-Vis) absorbance measurements were performed on Spark® Multimode Microplate reader. The absorption spectra were collected from 400 nm to 800 nm. As indicated in figures 3a and 3b, all prepared cit-AuNPs exhibited a strong surface plasmon resonance (SPR) absorption peak at around 520 nm.

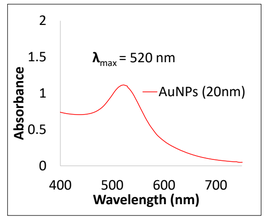

Figure 3a. UV-Vis absorption spectra for as-synthesized cit-AuNPs using citrate reduction method with size approximately 15 nm.

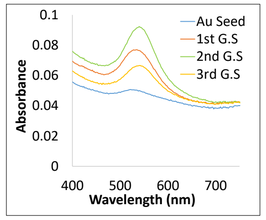

Figure 3b. UV-Vis absorption spectra for Au seed solution, and growth solutions 1st G.S, 2nd G.S, and 3rd G.S with sizes 25, 30, 40, and 60nm, respectively.

For BSA coated cit-AuNPs, all ultraviolet-visible (UV-Vis) absorbance measurements shows a gradual shift for surface plasmon resonance (SPR) absorption peak from 520 nm to 530 nm (Figure 4). Meanwhile, the % loading of BSA was measured based on the optical density (OD) using the following equation:

$$\text{Optical density (OD)} = \frac{A-B}{A} \text{ X } 100 \text{ ..... [5]}$$

Where, *A* is the absorbance of the ligand before conjugation, B is the absorbance of unbounded ligand in the supernatant (see figure5).

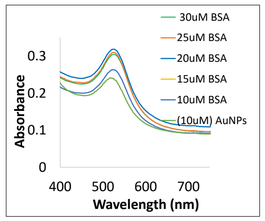

Figure 4. UV-Vis absorption spectra for BSA capped AuNPs. This capping indicated by the gradual shift of PSR peak from 520 nm to 530 nm.

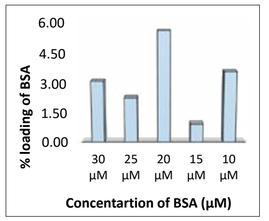

Figure 5. The % loading of BSA 3.11, 2.27, 5.61, 0.93, and 3.6 % with different concentrations 30, 25, 20, 15, and 10 µM, respectively.

Dynamic light scattering (DLS):

Size distribution by intensity (%), and zeta potential for cit-AuNPs in the presence & absence of BSA was observed by DLS as indicated in figures 6, and 7, respectively.

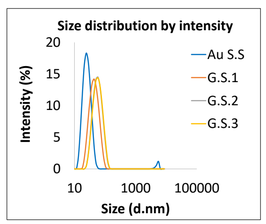

Figure 6. Size distribution by intensity (%) measured by DLS for Au seed solution, 1st G.S, 2nd G.S, and 3rd G.S with different sizes 25, 30, 40, and 60 nm, respectively, in the absence of BSA.

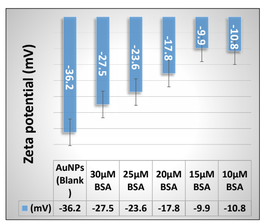

Figure 7. Zeta potential for AuNPs and BSA/AuNPs -36.2, -27.5, -23.6, -17.8, -9.9, and -10.8 at different concentrations 30, 25, 20, 15, and 10 µM, respectively.

Transmission electron microscopy (TEM):

As shown in both images 1a and 1b, the monodispersity and size of the as-prepared AuNPs were observed by means of transmission electron microscopy (TEM).

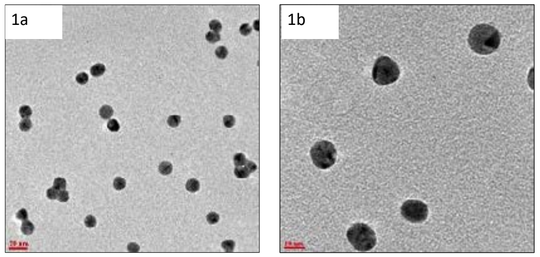

Image 1a, 1b. Transmission electron microscopy image of as-synthesized gold nanoparticles with an approximate size of 15 nm, while its concentration is about 1.46 × 10^8 NPs/mL.

Conclusion

A wide range of applications of AuNPs in medicine and biology has seen their use in genomic studies, biosensing, clinical chemistry, drug delivery, optical imaging etc. Despite such extensive field of studies, applications most commonly involve a single formulation with no comparison across size ranges. Molecular simulations, however, suggest that effectiveness can vary widely across different sizes, especially in the sub-10nm range, where particle curvature and size can influence loading, stability and transport efficiency. Our work, which is currently at an early stage of development, represent a systematic study of these effects.

References

[1] WHO, "COVID-19 Weekly Epidemiological Update Global epidemiological situation."

[2] Newyorktimes, "Coronavirus Vaccine Tracker- The new York times," 2020. [Online]. Available: https://www.nytimes.com/interactive/2020/science/coronavirus-vaccine-tracker.html. [Accessed: 19-Oct-2020].

[3] J. Chen et al., "Highly sensitive and visual detection of guanosine 3'-diphosphate-5'-di(tri)phosphate (ppGpp) in bacteria based on copper ions-mediated 4-mercaptobenzoic acid modified gold nanoparticles," Anal. Chim. Acta, vol. 1023, pp. 89–95, Sep. 2018, doi: 10.1016/j.aca.2018.02.082.

[4] R. Wu, H. Peng, J.-J. Zhu, L.-P. Jiang, and J. Liu, "Attaching DNA to Gold Nanoparticles With a Protein Corona," Front. Chem., vol. 8, p. 121, Feb. 2020, doi: 10.3389/fchem.2020.00121.

[5] P. Joshi et al., "Binding of chloroquine-conjugated gold nanoparticles with bovine serum albumin," J. Colloid Interface Sci., vol. 355, no. 2, pp. 402–409, 2011, doi: 10.1016/j.jcis.2010.12.032.

[6] C. Daruich De Souza, B. Ribeiro Nogueira, and M. E. C. M. Rostelato, "Review of the methodologies used in the synthesis gold nanoparticles by chemical reduction," J. Alloys Compd., vol. 798, pp. 714–740, 2019, doi: 10.1016/j.jallcom.2019.05.153.